First measurement of helicity-dependent cross sections in $\pi^0\eta$ photoproduction from quasi-free nucleons

A. Käser [a], M. Dieterle [a], L. Witthauer [a], S. Abt [a], P. Achenbach [b], P. Adlarson [b], F. Afzal [c], Z. Ahmed [d], J. Ahrens [b], J.R.M. Annand [f], H.J. Arends [b], M. Bashkanov [g], R. Beck [c], M. Biroth [b], N.S. Borisov [h], A. Braghieri [i], W.J. Briscoe [j], F. Cividini [b], C. Collicott [k], S. Costanza [i,1], A. Denig [b], E.J. Downie [b,j], P. Drexler [b], A. Fix [ℓ], S. Garni [a], D.I. Glazier [f,g], I. Gorodnov [h], W. Gradl [b], M. Günther [a], G.M. Gurevich [m], L. Heijkenskjöld [b], D. Hornidge [n], G.M. Huber [d], V.L. Kashevarov [b,h], S. Kay [g], I. Keshelashvili [a,2], R. Kondratiev [m], M. Korolija [o], B. Krusche [a], A.B. Lazarev [h], V. Lisin [m], K. Livingston [f], S. Lutterer [a], I.J.D. MacGregor [f], D.M. Manley [e], P.P. Martel [b,n], V. Metag [p], W. Meyer [q], R. Miskimen [r], E. Mornacchi [b], A. Mushkarenkov [m,r], A.B. Neganov [h], A. Neiser [b], M. Oberle [a], M. Ostrick [b], P.B. Otte [b], D. Paudyal [d], P. Pedroni [i], A. Polonski [m], S.N. Prakhov [b,s], G. Reicherz [q], G. Ron [t], T. Rostomyan [a,3], A. Sarty [k], C. Sfienti [b], V. Sokhoyan [b,j], K. Spieker [c], O. Steffen [b], I.I. Strakovsky [j], Th. Strub [a], I. Supek [o], A. Thiel [c], M. Thiel [b], A. Thomas [b], M. Unverzagt [b], Yu.A. Usov [h], S. Wagner [b], N.K. Walford [a], D.P. Watts [g], D. Werthmüller [a,f], J. Wettig [b], M. Wolfes [b], L. Zana [g]

[a] *Department of Physics, University of Basel, Basel, Switzerland*
[b] *Institut für Kernphysik, University of Mainz, Mainz, Germany*
[c] *Helmholtz-Institut für Strahlen- und Kernphysik, University of Bonn, Bonn, Germany*
[d] *University of Regina, Regina, SK S4S 0A2 Canada*
[e] *Kent State University, Kent, OH, USA*
[f] *SUPA School of Physics and Astronomy, University of Glasgow, Glasgow, G12 8QQ, UK*
[g] *SUPA School of Physics, University of Edinburgh, Edinburgh EEH9 3JZ, UK*
[h] *Joint Institute for Nuclear Research,141980 Dubna, Russia*
[i] *INFN Sezione di Pavia, Pavia, Italy*
[j] *Center for Nuclear Studies, The George Washington University, Washington, DC, USA*
[k] *Department of Astronomy and Physics, Saint Marys University, Halifax, Canada*
[ℓ] *Laboratory of Mathematical Physics, Tomsk Polytechnic University, Tomsk, Russia*
[m] *Institute for Nuclear Research, Moscow, Russia*
[n] *Mount Allison University, Sackville, New Brunswick E4L 1E6, Canada*
[o] *Rudjer Boskovic Institute, Zagreb, Croatia*
[p] *II. Physikalisches Institut, University of Giessen, Germany*
[q] *Institut für Experimentalphysik, Ruhr Universität, 44780 Bochum, Germany*
[r] *University of Massachusetts Amherst, Amherst, Massachusetts 01003, USA*
[s] *University of California at Los Angeles, Los Angeles, CA, USA*
[t] *Racah Institute of Physics, Hebrew University of Jerusalem, Jerusalem 91904, Israel*

Abstract

The helicity-dependent cross sections for the photoproduction of $\pi^0\eta$ pairs have been measured for the first time. The experiment was performed at the tagged photon facility of the Mainz MAMI accelerator with the combined Crystal Ball - TAPS calorimeter. The experiment used a polarized deuterated butanol target and a circularly polarized photon beam. This arrangement allowed the $\sigma_{1/2}$ (photon and target spin antiparallel) and $\sigma_{3/2}$ (parallel spins) components to be measured for quasi-free production of $\pi^0\eta$ pairs off protons and neutrons. The main finding is that the two helicity components contribute identically, within uncertainties, for both participant protons and neutrons. The absolute couplings for protons and neutrons are also identical. This means that nucleon resonances contributing to this reaction in the investigated energy range have almost equal electromagnetic helicity couplings, $A_{1/2}^{n,p}$ and $A_{3/2}^{n,p}$. Identical couplings for protons and neutrons are typical for Δ resonances and identical $A_{1/2}$ and $A_{3/2}$ components are only possible for $J \geq 3/2$ states, which constrains possible contributions of nucleon resonances.

1. Introduction

Excited states of the nucleon decay almost exclusively by the emission of mesons. Photoproduction of mesons is one of the principal tools for studying the nucleon excitation spectrum, which is crucial for the understanding of the strong interaction in the non-perturbative regime. So far, the data base for such reactions is dominated by single-meson production reactions. Two-body final states, such as πN, ηN,..., are still the backbone of most partial wave analyses, however, the progress in accelerator and detector techniques over the last two decades now allows studies of multi-meson production reactions with comparable statistical and systematic uncertainties. This advance has opened a new window on spectroscopy that provides access to new questions about the excitation spectrum of nucleons. The obvious nucleon resonances of interest are those states that, due to their internal structure, have only small branching ratios for direct decays to the nucleon ground state. Rather they decay predominantly in cascades involving at least one intermediate excited state. In the quark model, configurations with both oscillators excited are likely candidates for such patterns. This is discussed in Ref. [1] in context with the photoproduction of π^0 pairs through excitations of high lying nucleon resonances. However, even for medium high excitations such cascade decays can be very interesting when they allow one to study the states in detail which dominate the respective decay chain. Particularly interesting are final states with neutral mesons for which non-resonant background contributions are small.

The investigation of final states with meson pairs is challenging. The formalism discussing all possible observables for the photoproduction of single pseudoscalar mesons was laid out by Barker, Donnachie, and Storrow [2] and later Chiang and Tabakin [3] gave the final answer how many different observables have to be measured for a 'complete' experiment. In this case, differential cross sections, the three single polarization observables corresponding to a linearly polarized photon beam (Σ), a transversely polarized target (T), the polarization of the recoil nucleon (P), and several double polarization observables have to be measured as functions of two kinematic variables (usually incident photon energy E_γ or invariant mass W and meson center-of-momentum (cm) polar angle). In total eight observables, when combined in the right way, are sufficient. However, even this has not yet been achieved for the most prominent reaction channels like pion and η photoproduction.

The situation is more difficult for the production of meson pairs. This was discussed in detail by Roberts and Oed

Email address: bernd.krusche@unibas.ch (B. Krusche).
[1] also at Dipartimento di Fisica, Università di Pavia, Pavia, Italy.
[2] Now at Institut für Kernphysik, FZ Jülich, 52425 Jülich, Germany
[3] Now at Department of Physics and Astronomy., Rutgers University, Piscataway, New Jersey, 08854-8019, USA

[4]. The measurement of eight observables as functions of five kinematic parameters fixes only the magnitude of the amplitudes and 15 observables would be necessary to extract the complex phases also. This is certainly not practical, in particular not for reactions with small cross sections as production of $\pi\eta$ pairs. However, for specific questions already the measurement of one well chosen polarization observable can give useful additional information. For final states with meson pairs it is not always necessary to explore the full three-body structure of the final state. Already the analysis as a quasi two-body final state, for example $\gamma N \to N X$ ($X = \pi\eta$) can give valuable insights. Different partitions of the final state are also possible. An example for such an analysis is given in [5] for the production of $\pi\eta$ pairs off the nucleon measured with a linearly polarized photon beam. In this case, one can define polarization observables in analogy to [2,3] using the polar angle of the combined X particle system.

In spite of the complexity of photoproduction of meson pairs, double pion production has been intensively explored during the last decade. (see e.g. [1,6–11] and Ref. therein) but more recently the production of $\pi\eta$ pairs has also moved into the focus. This decay is more selective since the η meson, due to its isoscalar nature, can only be emitted in transitions between two isospin $I = 1/2$ $N^\star$ resonances or between two $I = 3/2$ Δ states. Cross-over decays between $N^\star$ and Δ states are not permitted. The data base for this reaction has grown rapidly during the last few years. Total cross sections, invariant-mass distributions, and some polarization observables, have been measured for the production of $\eta\pi^0$ pairs off protons at LNS in Sendai, Japan [12], GRAAL at ESRF in Grenoble, France [13], ELSA in Bonn, Germany [5,14–17], and at MAMI in Mainz, Germany [18–21] (see [22] for a summary). The isospin dependence of this reaction has been investigated at low incident photon energies ($E_\gamma < 1.4$ GeV) with measurements of the $\gamma d \to np\pi^0\eta$, $\gamma d \to nn\pi^+\eta$, $\gamma d \to pp\pi^-\eta$, and $\gamma d \to dp^0\eta$ reactions at MAMI [23,24]. For the quasi-free reactions, recoil nucleons detected in coincidence with the mesons were used to identify the final state.

Prior analyses of data for $\gamma p \to \pi^0\eta p$ have suggested the dominance of Δ excitations decaying via η emission to the $\Delta(1232)$ state [5,15,18,19]. Some minor contributions were attributed to the $R \to S_{11}(1535)\pi$ intermediate state ($R =$ any nucleon resonance), and at higher incident photon energies, to the decay of the a_0 meson. The isospin dependence [23,24] was in excellent agreement with the assumption of the reaction chain $\gamma N \to \Delta\eta \to N\pi\eta$. This means that the cross sections for the production of the same charge type of pions (neutral or charged) for proton and neutron targets were identical within uncertainties. The cross sections for the production of neutral pions were, for both types of incident nucleons, twice as large as for charged pions. The same relations also hold for the decay of a primarily excited Δ res-

onance, via pion emission to an $N^\star$ state, with subsequent η decay to the nucleon ground state. However, invariant-mass distributions of the meson-nucleon pairs favor the $\Delta(1232)\eta$ intermediate state [24]. The isobar model analysis of Fix and coworkers [25] identified major contributions from the D_{33} partial wave as the initial state ($\Delta(1700)3/2^-$ and $\Delta(1940)3/2^-$ resonances). The comprehensive analysis of differential cross sections and polarization observables in [5] quotes not only branching ratios into $\Delta(1232)\eta$ for the $\Delta(1700)3/2^-$, $\Delta(1900)1/2^-$, $\Delta(1905)5/2^+$, $\Delta(1910)1/2^+$, $\Delta(1920)3/2^+$, and $\Delta(1940)3/2^-$ states, but also branching ratios into $N(1535)\pi$.

The present paper reports the results for the first measurement of any double polarization observable for this reaction. Measured was the observable E (see definition below), and the decomposition of the cross section σ into its helicity-1/2 and helicity-3/2 parts, $\sigma_{1/2}$ and $\sigma_{3/2}$. This is the first measurement of the helicity structure for photoproduction of $\pi^0\eta$ pairs from quasi-free protons and neutrons. Even for free protons this observable has not yet been studied. It is measured with a longitudinally polarized target and a circularly polarized photon beam, where $\sigma_{3/2}$ corresponds to parallel target-nucleon and photon-beam spin orientation and $\sigma_{1/2}$ to the anti-parallel orientation. The electromagnetic excitation of nucleon resonances in the S_{11}, S_{31} and P_{11}, P_{31} partial waves can only contribute to the $\sigma_{1/2}$ part, while nucleon resonances with larger spins may contribute to both $\sigma_{1/2}$ and $\sigma_{3/2}$. The measurement of the helicity decomposition for the latter is sensitive to the relative contribution of the $A_{3/2}$ and $A_{1/2}$ electromagnetic amplitudes of resonance excitations. These are important properties of the structure of the excited nucleon states predicted e.g. by quark models.

The two states, $\Delta(1700)3/2^-$ and $\Delta(1940)3/2^-$, suggested by several analyses of existing data as dominant in the reaction up to invariant masses of 1.9 GeV, are both listed in the *Review of Particle Physics* (RPP) [26] with similar $A_{3/2}$ and $A_{1/2}$ couplings. The RPP estimates for the Breit-Wigner photon-decay amplitudes for the $\Delta(1700)3/2^-$ are $A_{1/2} = A_{3/2} = 140 \pm 30$ (all values for photon couplings in units of $10^{-3}\text{GeV}^{-1/2}$). The most recent results come from the Bonn-Gatchina (BnGa) coupled channel analysis for π^0 pairs [1] and $\pi^0\eta$ pairs [5]. Both papers quote values of $A_{1/2} = 165 \pm 20$ and $A_{3/2} = 170 \pm 25$. Previous analyses listed in RPP [26] differ significantly in absolute values (for example between 58 and 226 for $A_{1/2}$) and partly also in the $A_{3/2}/A_{1/2}$ ratio. The RPP lists for the $\Delta(1940)3/2^-$ state only results from the BnGa analysis [1,5], which are $A_{1/2} = 170^{+110}_{-80}$ and $A_{3/2} = 150 \pm 80$, so that in this case the uncertainty of the $A_{3/2}/A_{1/2}$ ratio is still large. All these results come mostly from coupled-channel analyses of data which are not directly sensitive to the $\sigma_{3/2}/\sigma_{1/2}$ ratio (but only rather indirectly sensitive via angular distributions etc.). The present experiment provides the first direct measurement of this ratio.

2. Polarization observable E and helicity dependent cross sections $\sigma_{1/2}$ and $\sigma_{3/2}$

The polarization observable E and the helicity-dependent cross sections $\sigma_{1/2}$ and $\sigma_{3/2}$ can be measured with a circularly polarized photon beam of polarization $P_\odot$ and a longitudinally polarized target of polarization P_T. The cross sections $\sigma_{1/2}$ and $\sigma_{3/2}$ correspond to the antiparallel ($\uparrow\downarrow$) or parallel ($\uparrow\uparrow$) configurations of incident nucleon and photon spin (details of the spin-helicity configurations are for example given in [29]). In the full three-body formalism of [4] this would be the observable $P_z^\odot$. However, since we analyze only the fully integrated asymmetry, for which the definition is identical to the analysis of a two-body final state, as a short-hand notation we use 'E' as in [2]. The asymmetry and the two partial cross sections are then defined by

$$E = \frac{\sigma_{1/2} - \sigma_{3/2}}{\sigma_{1/2} + \sigma_{3/2}} = \frac{1}{P_\odot P_T} \cdot \frac{N_{1/2} - N_{3/2}}{(N_{1/2} - N_B) + (N_{3/2} - N_B)} .$$
(1)

The right-hand side of the equation with the count rates $N_{1/2}$ and $N_{3/2}$, measured for the two spin configurations, ensures that all absolute normalizations (target density, beam flux, detection efficiencies,...) cancel in the count-rate ratio. Since molecular hydrogen cannot be polarized, solid deuterated butanol ($C_4D_{10}O$) was used as the target material. Therefore, a background count rate N_B from reactions with nucleons bound in the unpolarized $J = 0$ carbon and oxygen nuclei must be subtracted in the denominator. This background cancels in the cross section difference in the numerator.

There are different strategies for extracting the asymmetry E and $\sigma_{1/2}$ and $\sigma_{3/2}$ from a measurement with a butanol target. For the asymmetry E, in one approach, the denominator ($\sigma_{1/2} + \sigma_{3/2}$) was replaced by the results from a measurement of the unpolarized cross section σ_0 with a liquid deuterium target using $2\sigma_0 = \sigma_{1/2} + \sigma_{3/2}$. This method needs absolutely normalized cross-section data for numerator and denominator. These results are labeled (A). For the second method, a measurement was performed to determine the background rate N_B with a carbon foam target that had the same mass, volume, and density as the non-deuterium components of the butanol target. A small correction had to be applied for nucleons bound in oxygen nuclei because nuclear cross sections scale as $A^{2/3}$ rather than A. This method required only that the count rates measured with the butanol and the carbon foam were normalized to the beam flux. The results from this analysis are labeled (B). The systematic uncertainties of the two methods have different sources. However, the statistical uncertainties are highly correlated because they are dominated by the fluctuations of the small numerator, which is identical in both analyses.

For the cross sections $\sigma_{1/2}$ and $\sigma_{3/2}$, three different ways of extraction were explored. They are all based on the relations

$$\sigma_{1/2} = \sigma_0 \cdot (1 + E)$$
$$\sigma_{3/2} = \sigma_0 \cdot (1 - E) \, , \qquad (2)$$

but different results were used for E and σ_0.

- Version (1): E was taken from analysis (A) (denominator from measurement with liquid deuterium target) and σ_0 also from the measurement with the unpolarized target.
- Version (2): E was taken from analysis (B) (carbon subtraction), but σ_0 again from the liquid deuterium target.
- Version (3): E and σ_0 were taken from carbon subtracted butanol data.

3. Complications for quasi-free production off bound nucleons

Measurements for nucleons bound in light nuclei, which are necessary for neutrons, introduce some complications. A trivial experimental one is the requirement to detect the recoil nucleons, which for neutrons in particular, reduces the detection efficiency.

Nuclear Fermi motion smears structures in excitation functions and angular distributions. However, this problem can be partly avoided by a complete reconstruction of the kinematics of the final state. For photoproduction off the deuteron, the final state is completely determined kinematically, within experimental resolution, when the four momenta of all produced mesons and the three-momentum direction of the recoiling nucleon are measured [30]. In this case, only the kinetic energy of the recoil nucleon and the three momentum of the spectator nucleon (four parameters) are missing. These parameters can be reconstructed from energy and momentum conservation (four equations). This analysis determines the 'true' center-of-momentum (cm) energy $W = \sqrt{s}$ in the incident-photon - participant-nucleon system. The obtained resolution for W is poorer than that obtained with measurements with free proton targets for which W can be directly reconstructed from the incident photon energy, but this is not a problem for smoothly varying cross sections. All values for W used in this analysis have been reconstructed using this method.

More problematic are effects of final-state interactions (FSI) between the nucleons, between mesons and nucleons, and, for multi-meson production reactions, also between mesons. The comparison of cross sections measured for the photoproduction of $\pi^0\eta$ pairs off free protons and off bound protons [23,24] shows that such effects are relevant for this final state. On an absolute scale, free and quasi-free cross sections deviate on average by $\approx$30%. Model calculations of such effects are difficult and not far advanced. Recently, some results were published for estimates of FSI effects for differential cross sections in single pion and η production [31,32]. They were, however, not yet precise enough for numerical corrections of measured data, clearly more efforts in theory are needed. Similar effects in the production of meson pairs and for polarization observables are almost unexplored in model calculations. However, there are some interesting experimental results from the comparison of pho-

toproduction reactions off free protons and quasi-free protons bound in the deuteron. As mentioned above, differential cross sections for $\eta\pi$ production are significantly different for free and quasi-free protons, cross sections for single π^0 production are even more different in some energy regions [36,38], also the results for pion pairs differ up to 20%, while effects in η production are insignificant. This means that FSI effects on absolute cross sections are strongly reaction dependent. However, polarization observables seem to be effected in a completely different way. We have previously tested this for the polarization observable $I^{\odot}$ measured with a circularly polarized photon beam on unpolarized target for the production of meson pairs [24,27,28]. No significant effects were found for $\pi\pi$ and $\pi\eta$ pairs. Also, for the helicity asymmetry E, as defined in this paper, no effects were found for single π^0 [37] and η production [33–35], although the effects on absolute cross sections for π^0 production are substantial. For $\pi\eta$ production also shapes of invariant mass distributions of meson-meson and meson-nucleon pairs are basically unaffected [24].

Therefore, one expects significant FSI effects for the absolute scale of the $\sigma_{1/2}$ and $\sigma_{3/2}$ cross sections, but only minor effects for E and the $\sigma_{3/2}/\sigma_{1/2}$ cross-section ratio. Unfortunately, since double polarization data of this type are not yet available for free protons, this cannot be tested directly.

4. Experimental Setup

The present results are based on the same data set that was previously used to extract the polarization observable E for the production of η mesons [33,34] and for π^0 mesons [37] off quasi-free nucleons (most details are given in [34]). Therefore, we give only a short summary of the experimental details.

The measurements were performed at the electron accelerator MAMI in Mainz, Germany [40]. The electron source was an optically pumped gallium-arsenide-phosphor (GaAsP) photocathode [39] delivering polarized electrons. During four beam times, which were analyzed for the present results, the electrons were accelerated to energies close to 1.6 GeV in the accelerator stages of MAMI. The high energy electrons produced bremsstrahlung in a Co-Fe alloy (Vacoflux50, 10 μm thickness) and in this process the longitudinally polarization of the electrons was transferred to circular polarization of the photons according to [41]:

$$P_\gamma = P_{e^-} \cdot \frac{4x - x^2}{4 - 4x + 3x^2} \, , \qquad (3)$$

where P_{e^-} and P_γ are the degrees of polarization of the electrons and the photons, respectively, and $x = E_\gamma/E_{e^-}$. The electron polarization was measured periodically with a Mott polarimeter close to the electron source and monitored with a Møller polarimeter viewing the ferromagnetic bremsstrahlung foil. Both results were in good agreement and the average electron polarization was $P_{e^-} \approx 83\%$.

4

The photon beam was energy tagged with the Glasgow spectrometer [42] with a typical resolution of 4 MeV, which results from the widths of the 353 plastic scintillators used in the focal plane detector for detection of the post-bremsstrahlung electrons. This detector covers 5 - 93% of the incident electron energies but the part corresponding to high electron energies (low photon energies) was deactivated to increase counting statistics for high-energy photons. The active photon-energy range spanned from $E_\gamma \approx$ 400 MeV to 1450 MeV.

The photon beam size was defined by a collimator with 2 mm diameter, producing a beam-spot diameter of 9 mm on the production target. The longitudinally polarized target had a diameter of 19.8 mm and a length of 20 mm. It consisted of butanol beads of average diameter ≈1.9 mm [43]. The deuterons in the butanol molecules were polarized by Dynamic Nuclear Polarization (DNP) [44] in a strong magnetic field (1.5 T) at a temperature of 25 mK. After the target had been polarized, the polarizing magnet was replaced by a small solenoidal holding coil with a magnetic field of 0.6 T. Relaxation times of more than 2000 h and polarization degrees around 60% were achieved.

However, as discussed in detail in [33,34] the target polarization was not homogeneous across the target diameter for the first three beam times. Thus, the standard NMR measurements of the polarization did not correspond to the effective polarization in the target center hit by the photon beam. The problem was due to small inhomogeneities of the field of the 1.5 T magnet, used for the DNP process, combined with the very narrow NMR resonance of deuterated butanol doped with trityl-radicals. The fourth beam time used a less sensitive radical (Tempo), which resulted in lower polarization (55%) that, however, could be determined much more accurately. The polarization of all beam times were then recalibrated to the last beam time using the measured asymmetries for the photoproduction of η-mesons.

Furthermore, the NMR measurements determine only the polarization of the deuterium nuclei. For the effective polarization of the nucleons bound in the deuteron one must take into account the d-wave component in the deuteron wave function. This results in a downward correction of the measured polarization degrees on the order of 8% [45].

The experimental setup, combining the Crystal Ball and TAPS detectors with additional devices for charged particle identification, was identical to the one used for the results reported in [33,34,37], which used the same data set. The electromagnetic calorimeter combined the Crystal Ball (CB) [46] and TAPS [47] detectors. The first (672 NaI(Tl) crystals) covered the solid angle for polar angles between 20° and 160° and the second (384 BaF$_2$ crystals) covered as a forward wall polar angles between 5° and 21°. A cylindrically shaped charged-particle identification detector (PID) [48], consisting of 24 plastic scintillators, was mounted inside the CB around the target and a 5 mm thick plastic scintillator was mounted in front of each BaF$_2$ crystal for charged particle identification (CPV detector).

The experimental trigger was based on a hit-cluster multiplicity condition for hits in the combined calorimeter and a sum threshold for the total energy deposition in the CB. Only events with at least two cluster hits in the calorimeter were selected. Since each hit activates an a priori unknown number of detector modules, this condition was approximately imposed by dividing TAPS azimuthal coverage into six equal triangular sectors and the CB into sectors of 16 adjacent modules. Only events that activated at least two sectors were accepted. Furthermore, it was required that the analog sum of the energy signals from the CB exceeded 250 MeV. This condition removed a large fraction of electromagnetic background in the calorimeter. Events from single π^0 decays, with both photons in TAPS, were thus not included in the trigger, but this is irrelevant for the $\pi^0\eta$ final state. In the offline analysis, event-selection conditions considered only meson-decay photons. This avoided systematic uncertainties from the unpredictable energy deposition of recoil neutrons in the calorimeter.
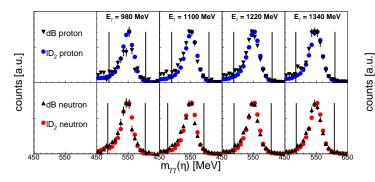
5. Data Analysis

The data analysis was based on the methods developed for the reaction identification of meson pairs ($\pi\pi$ and $\pi\eta$) described in detail in [7,23,24,27,28] for measurements with unpolarized liquid deuterium targets. The treatment of the unpolarized background from 'heavy' nuclei (carbon, oxygen), present in the butanol target, is described in [33,34,37] for photoproduction of η and π^0 mesons. For the latter, in addition to the data from the polarized butanol target, measurements with a carbon foam target and a liquid deuterium target were analyzed.

All detector modules were calibrated for their energy and timing response as discussed in detail in [38]. Background from random coincidences with the tagger was subtracted as discussed in [49]. In the first step of particle identification, hits in the calorimeter were classified as 'charged' or 'neutral' depending on the response of the PID and the CPV. Subsequently, for hits in TAPS, pulse-shape analysis (PSA) and time-of-flight versus energy analysis were used for the separation of photons from protons and neutrons as in [24,38]. The only remaining ambiguity was that photons and neutrons in the CB cannot be distinguished event-by-event (see e.g. [49,50]) by the detector response. The timing resolution is only modest due to the short time-of-flight distance, PSA methods cannot be applied, and cluster-size distributions discriminate not on an event-to-event basis.

Events accepted for further analysis were those with four neutral and one charged hit for the $\gamma d \to \pi^0\eta p(n)$ reaction and five neutral hits for the $\gamma d \to \pi^0\eta n(p)$ reaction (nucleons in parentheses are undetected spectators).

As discussed in detail in [24], neutral hits in the CB were assigned to photons or neutrons using a χ^2 analysis. For events with four or five neutral hits, the invariant masses of all possible pair combinations were compared to the π^0 and η masses. The χ^2 was defined by
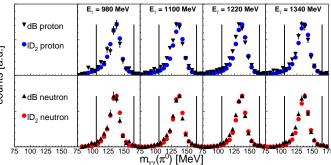
5

Fig. 1. Left-hand side: Invariant-mass distributions of the photon pairs assigned to decays of the η mesons. Upper row: coincidence with recoil protons, lower row: coincidence with recoil neutrons. Centers of energy bins at 980 MeV, 1100 MeV, 1220 MeV, and 1340 MeV. Vertical lines indicate the experimental cuts. Filled spheres: results for liquid deuterium target, black triangles: butanol target. Right-hand side: Invariant-mass distributions of the photon pairs assigned to π^0 decays. Notation as for left-hand side.

$$\chi^2(k) = \sum_{i=1}^{2} \left(\frac{m_{\pi^0,\eta} - m_{i,k}}{\Delta m_{i,k}} \right)^2 \quad \text{with} \quad k = 1,..,n_p, \quad (4)$$

where the $m_{i,k}$ are the invariant masses of the i-th pair in the k-th permutation of the hits and $\Delta m_{i,k}$ is the corresponding uncertainty from the experimental energy and angular resolution. Both were computed event-by-event. For events with exactly four neutral hits, this analysis was used only to find the most probable combination of the four decay photons relating to a parent π^0 and η. For events with five neutral hits, the remaining hit was assigned to the neutron. In order to suppress combinatorial background, the hypothesis of $\pi^0\pi^0$ pairs was also tested and the event was discarded when such a combination resulted in a smaller χ^2 than any of the $\pi^0\eta$ hypotheses. One-dimensional projections of the two-dimensional $\eta - \pi$ invariant mass spectra are shown in Fig. 1. As expected, the results for the liquid deuterium and the solid butanol targets are practically identical, in spite of the heavy-nuclei background in the butanol spectra, because Fermi motion does not influence invariant masses.
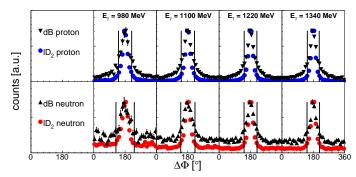

Fig. 2. Coplanarity spectra. Upper row: coincidence with recoil protons, lower row: coincidence with recoil neutrons for the same energy ranges as Fig. 1 and with same notation.

Background not eliminated by the invariant mass analysis can arise for the liquid deuterium and butanol targets from photoproduction of π^0 pairs or other reactions with multi-photon final states. For the butanol target, background can also arise from reactions with the nucleons bound in the unpolarized nuclei. Due to the larger Fermi

momenta in heavier nuclei, this leads to a larger width of the signal. Such backgrounds can be removed by analyses of the reaction kinematics. The most basic condition is the coplanarity of the two mesons and the recoil nucleon. Due to momentum conservation, the difference in the azimuthal angle $\Delta\Phi$ between the $\eta\pi^0$ pair and the recoil nucleon must be 180°. This is normally not the case when additional particles have escaped detection or four photons have been wrongly assigned to the decay of a π^0 and an η meson. The coplanarity spectra shown in Fig. 2 show a clear peak at 180° and only events between ±36° around the peak were accepted.

Even more powerful is the analysis of the missing mass. For this analysis, the recoil nucleon was treated as a missing particle (although it was detected) and its mass was calculated from the four momenta of the incident photon P_γ, the initial-state nucleon P_N, the final-state pion P_{π^0}, and the η meson P_η:

$$\Delta M = |P_\gamma + P_N - P_\pi - P_\eta| - m_N , \quad (5)$$

where the nucleon mass m_N was subtracted so that true $\gamma N \to N\pi^0\eta$ events were expected at $\Delta M = 0$. In Eq. 5, P_N is unknown due to the contribution of the Fermi momentum to the four momentum. The Fermi momentum was set to zero. This results in a broadening of the ΔM distribution which is more important for reactions with nucleons bound in the heavier nuclei than for the nucleons from the deuteron. This analysis was done for the butanol, the liquid deuterium, and the carbon foam target. As discussed in [33,34,37] for other final states, the spectra from all three targets were normalized absolutely on the basis of photon flux, target density, etc. and are compared in Fig. 3. The sum of the liquid deuterium and carbon data agree well with the butanol data so that the contribution of reactions on quasi-free nucleons in deuterium can be precisely determined for the measurement with the butanol target. This was only important for analysis (B) of the asymmetry E, for which the denominator was taken from the measurement with the butanol target. For analysis (A), only the difference between the two helicity states in the numerator was used, for which the unpolarized carbon background
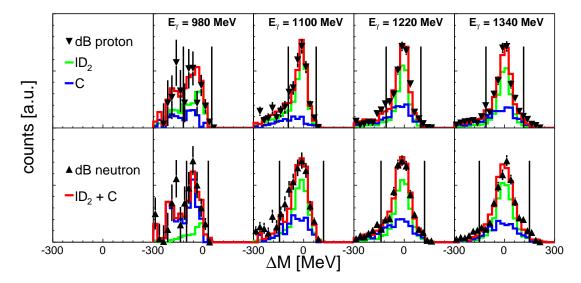
Fig. 3. Missing-mass spectra extracted from Eq. 5. Black triangles: butanol target, green histograms: liquid deuterium target, blue histograms: carbon foam target, red histograms: sum of liquid deuterium and carbon foam. Upper row: coincidence with recoil protons, lower row: coincidence with recoil neutrons. Vertical lines: analysis cuts.

cancels and the denominator was taken directly from the measurement with the liquid deuterium target.

The measured yields were normalized absolutely with respect to the incident photon flux, the target density, the π^0 and η decay branching ratios into two photons [26], and the detection efficiency. The detection efficiency was determined with Monte Carlo (MC) simulations which employ the Geant4 [51] tool kit. As discussed in [24], the generator of reaction-kinematics input into the simulation was based on the dominant $\Delta^\star \to \Delta(1232)\eta \to N\eta\pi^0$ decay chain. It included the effects from the Fermi motion of the bound nucleons using the Paris-potential parameterization for the deuteron wave function in momentum space [52]. However, the effects of Fermi motion were mostly eliminated by the kinematic reconstruction of the final state. The MC simulations are precise and reliable for the detection of photons. There were, however, imperfections in the MC for the detection of recoil nucleons where these particles were emitted into the transition area between CB and TAPS. There inert materials from support structures, cables, etc. were not implemented in the MC with sufficient accuracy. Therefore, as in [37,49], corrections based on the analysis of reactions such as $\gamma p \to p\eta$ and $\gamma p \to n\pi^0\pi^+$ measured with a liquid hydrogen target were applied. However, they mostly cancel in the asymmetries.

All results are given as a function of the reconstructed invariant mass W defined as:

$$W = \sqrt{s} = |P_\pi + P_\eta + P_N|, \qquad (6)$$

where P_π, P_η, and P_N, are the four momenta of the π^0, the η, and the recoil nucleon, respectively. The four momenta of the pion and the eta were obtained from the decay photons measured in the calorimeter, while the four momentum of the recoil nucleon was defined by its measured azimuthal and polar angles as well as overall momentum and energy conservation (see e.g. [24,30,33,49]).

The systematic uncertainty of the asymmetry is dominated by the uncertainty of the polarization of the photon beam (2.7%) and the target (10%) [34]. The latter was very conservatively estimated due to the necessary recalibration of the first three beam times. Most other uncertainties cancel in the ratio of Eq. 1. Only higher-order effects from either the normalization to data from the measurement with a liquid deuterium target or the subtraction of the carbon background in the denominator can contribute. This means that only the difference between systematic effects for the three target types matters. Consequently, photon and recoil nucleon detection efficiencies and kinematic cuts are much less important than for absolute cross-section measurements. Systematic effects are further reduced in the comparison of the asymmetry for recoil protons and neutrons.

The $\sigma_{1/2}$ and $\sigma_{3/2}$ cross sections also carry the uncertainty from the absolute normalization (photon flux, target density), estimated to be between 5% - 7% [23,24,37], and uncertainties from the MC simulations of detector acceptance estimated in the range 5% - 10%. However, these uncertainties largely cancel in the comparison of the two helicity cross sections.

6. Results

The results for the double polarization observable E (see Eq. 1) are shown in Fig. 4 as a function of the invariant mass W. The results from the two different analyses using either a normalization to the unpolarized cross section measured with a liquid deuterium target (analysis (A)) or the subtraction of the unpolarized carbon background in the denominator of Eq. 1 (analysis (B)) are in good agreement, which demonstrates that systematic effects from normalizations and background subtraction are well under con-
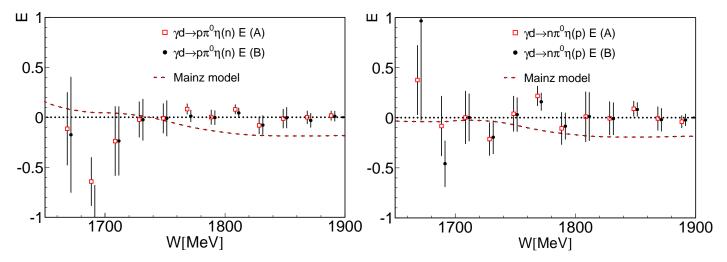
Fig. 4. Double polarization observable E. Left-hand side: quasi-free protons, right-hand side: quasi-free neutrons. Open (red) symbols: analysis (A) (normalization to unpolarized deuterium cross sections), closed (black) symbols: analysis (B) (subtraction of carbon background). Data points shifted by ± 1.5 MeV from their nominal values for better readability of the figure. Dashed lines: predictions from the Mainz model [21].

trol. The statistical fluctuations of both analyses are highly correlated. This was expected because the fluctuations are dominated by the almost vanishing numerator of the ratio in Eq. 1, which was identical for both analyses.

The result for the asymmetries is different from other reaction channels such as η production [33,34] and π^0 production [37]. The asymmetry vanishes, within statistical uncertainties, over the full investigated energy range. The vanishing asymmetry is certainly not an instrumental effect because the same data set has already produced substantial asymmetries for production of η mesons [33,34], single π^0 production [37], and production of pion pairs (not yet published). This means that contributions to $\eta\pi^0$ production must be almost exactly balanced for the excitation of nucleon resonances via the $A_{1/2}$ and $A_{3/2}$ electromagnetic reaction amplitudes. This result was established for reactions off protons and off neutrons as expected for the primary excitation of Δ resonances. The most recent results for this reaction from an analysis of cross section data and photon-helicity asymmetries (circularly polarized photon beam, unpolarized target) in the framework of the Mainz model have been published in Ref. [21] (the basis of this model is discussed in [25]). The model predictions for the E asymmetry are plotted in Fig. 4. In the region of the strongly contributing $\Delta(1700)3/2^-$ resonance agreement is reasonable within the relatively large statistical uncertainties of the experimental data. At larger invariant masses, the predictions favor a negative asymmetry and deviate systematically from the measured vanishing asymmetries. This deviation is even more apparent in the comparison of the helicity-dependent cross sections in Fig. 6.

The helicity-dependent cross sections from the three different analyses for coincident recoil protons and neutrons are summarized in Fig. 5. The three analyses agree within statistical uncertainties, which indicates that there are no serious systematic effects, either from the use of the unpolarized cross section measured with a liquid deuterium

target, or from the carbon subtraction. The agreement of analysis (3) with the other two results means that not only the asymmetries, but also the absolute cross section, can be extracted from the carbon-subtracted butanol data.
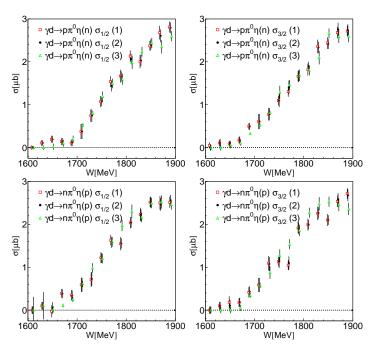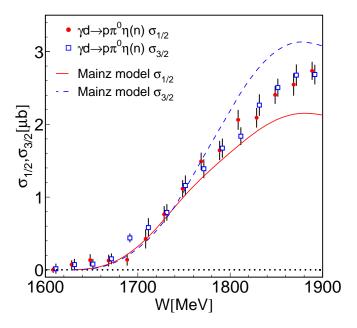

Fig. 5. Helicity-dependent cross sections $\sigma_{1/2}$ (left-hand side) and $\sigma_{3/2}$ (right-hand side) for quasi-free protons (upper row) and quasi-free neutrons (bottom row) for the three different analysis methods. version (1): (red squares): E from analysis (A), σ_0 from unpolarized deuterium cross section, version (2): (black filled dots): E from analysis (B), σ_0 from unpolarized deuterium cross section, version (3): (green triangles): E from analysis (B), σ_0 also from butanol target with carbon subtraction. Data points for (2) at nominal values, points for (1),(3) shifted by ± 1.5 MeV.

The results from the three analyses were averaged for the final results of the helicity-dependent cross sections, which are shown in Fig. 6. Since the statistical fluctuations of the
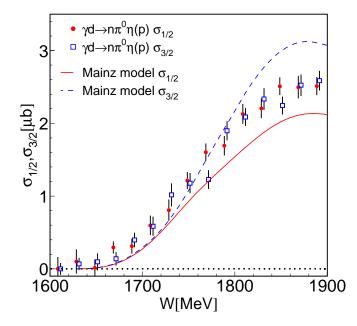
Fig. 6. Helicity-dependent cross sections $\sigma_{1/2}$ (filled red dots) and $\sigma_{3/2}$ (open blue squares) as function of total cm energy W. The results from the three different analyses (see Fig. 5) have been averaged. Left-hand side: coincidence with recoil protons, right-hand side: coincidence with recoil neutrons. Data points shifted by ± 1.5 MeV from their nominal values. Solid (red) lines and dashed (blue) lines: results from the Mainz model [21]. All model curves are scaled down by a common factor of 1.3 to account for FSI effects.

three extractions are strongly correlated due to the correlation of the numerator for analysis (A) and (B) of the asymmetry E and the use of σ_0 from the liquid deuterium target for analysis (1) and (2), the statistical uncertainties were combined linearly, rather than quadratically. The main result is that for quasi-free protons, as well as for quasi-free neutrons, the two helicity cross sections $\sigma_{1/2}$ and $\sigma_{3/2}$ agree within statistical uncertainties. Also, as expected from the results in [23], the results for the neutron and the proton are almost identical in magnitude. One should, however, note that the results for the total unpolarized cross section for the quasi-free proton are affected by FSI as discussed in [23,24]. Compared to reactions on the free proton, cross sections are lower by approximately 30%. The results are compared to the model predictions from [21]. All model results have been scaled down by a factor of 1.3 to account for the reduction of the quasi-free cross sections in absolute magnitude with respect to free-nucleon cross sections as observed in [24]. The comparison emphasizes what can already be seen in Fig. 4. In the energy range around 1700 MeV, dominated by the $\Delta(1700)3/2^-$ resonance, experimental data and model predictions agree in so far as the two helicity dependent cross sections are equal within uncertainties (Ref. [21] quotes an $A^{3/2}/A^{1/2}$ ratio of 0.8). Small deviations between experimental data and model results on an absolute scale may be due to the rough 30% correction of FSI effects which may also have some energy dependence. However, at invariant masses above 1750 MeV the model predicts a clear dominance of the $\sigma_{3/2}$ part of the cross section, which is not seen in the measured data. In the model fit, this arises from large $A^{3/2}/A^{1/2}$ ratios for the $\Delta(1920)3/2^+$ and the $\Delta(1940)3/2^-$ states. These ratios were smaller in the original version of this model [25]

(see Table I in [21]) and they were much smaller in the BnGa model [5] but increased in the more recent Mainz fit of several differential cross sections [21].

7. Summary and Conclusions

The double-polarization observable E and the helicity-dependent cross sections $\sigma_{1/2}$ and $\sigma_{3/2}$ were measured for photoproduction of $\pi^0\eta$ pairs from quasi-free protons and neutrons. As already reported in [23,24], the reactions off protons and neutrons have almost exactly identical cross sections. Compared on an absolute scale to the free-proton cross sections, they are, however, significantly reduced due to FSI effects. The first measurement of the helicity dependence shows in addition that for both target nucleons the asymmetry E is consistent with zero. This means that contributions from the two helicity states must be exactly balanced over the full energy range explored. The most natural explanation for both observations is that this reaction is dominated by the excitation of one (or few) Δ resonances decaying via η emission to the $\Delta(1232)$ with subsequent pion decay to the nucleon ground state and that the electromagnetic excitation amplitudes of the primarily excited Δ states are nearly identical for both helicity states. The new data will certainly much constrain future partial wave analyses in this energy range. Comparison to existing model predictions shows that the ratio of the so far poorly known $A_{1/2}/A_{3/2}$ helicity couplings for the higher lying Δ states must be almost certainly revised. The RPP [26] values for this parameters have still large uncertainties, which probably cover the range of needed modifications, but the present data will constrain them much tighter.

Acknowledgments

References

[1] V. Sokhoyan et al., Eur. Phys. J. A 51 (2015) 95.
[2] L.S. Barker, A. Donnachie, J.K. Storrow, Nucle. Phys. B 95 (1975) 347.
[3] W.T. Chiang, F. Tabakin, Phys. Rev. C 55 (1997) 2054.
[4] W. Roberts and T. Oed, Phys. Rev. C 71 (2005) 055201.
[5] E. Gutz et al., Eur. Phys. J. A 50 (2014) 74.
[6] A. Thiel et al., Phys. Rev. Lett. 114 (2015) 091803.
[7] M. Dieterle et al., Eur. Phys. J. A 51 (2015) 142.
[8] V. Kashevarov et al., Phys. Rev. C 85 (2012) 064610.
[9] F. Zehr et al., Eur. Phys. J. A 48 (2012) 98.
[10] A.V. Sarantsev et al., Phys. Lett. B 659 (2008) 94.
[11] U. Thoma et al., Phys. Lett. B 659 (2008) 87.
[12] T. Nakabayashi et al., Phys. Rev. C 74 (2006) 035202.
[13] J. Ajaka et al., Phys. Rev. Lett. 100 (2008) 052003.
[14] I. Horn et al., Phys. Rev. Lett. 101 (2008) 202002.
[15] I. Horn et al., Eur. Phys. J. A 38 (2008) 173.
[16] E. Gutz et al., Eur. Phys. J. A 35 (2008) 291.
[17] E. Gutz et al., Phys. Lett. B 687 (2010) 11.
[18] V. Kashevarov et al., Eur. Phys. J. A 42 (2009) 141.
[19] V. Kashevarov et al., Phys. Lett. B 693 (2010) 551.
[20] J.R.M. Annand et al., Phys. Rev. C 91 (2015) 055208.
[21] V. Sokhoyan et al., Phys. Rev. C 97 (2018) 055212, and A. Fix, private communication.
[22] B. Krusche and C. Wilkin, Prog. Part. Nucl. Phys. 80 (2015) 43.
[23] A. Käser et al., Phys. Lett. B 748 (2015) 244.
[24] A. Käser et al., Eur. Phys. J. A 52 (2016) 272.
[25] A. Fix et al., Phys. Rev. C 82 (2010) 035207.
[26] C. Patrignani et al., Chin. Phys. C 40 (2016) 100001.
[27] M. Oberle et al., Phys. Lett. B 721 (2013) 237.
[28] M. Oberle et al., Eur. Phys. J. A 50 (2014) 54.
[29] D. Drechsel and L. Tiator, Annu. Rev. Nucl. Part. Sci. 54 (2004) 69.
[30] B. Krusche, Eur. Phys. J. Special Topics 198 (2011) 199.
[31] V.E. Tarasov et al., Phys. of Atomic Nuclei 79 (2016) 216.
[32] S.X. Nakamura, H. Kamano, T.-S. H. Lee, and T. Sato arXiv:1804.04757 (2018).
[33] L. Witthauer et al., Phys. Rev. Lett. 117 (2016) 132502.
[34] L. Witthauer et al., Phys. Rev. C 95 (2017) 055201.
[35] L. Witthauer et al., Eur. Phys. J. A 53 (2017) 58.
[36] M. Dieterle et al., Phys. Rev. Lett. 112 (2014) 142001.
[37] M. Dieterle et al., Phys. Lett. B 770 (2017) 523.
[38] M. Dieterle et al., Phys. Rev. C 97 (2018) 065205.
[39] K. Aulenbacher et al., Nucl. Instr. Meth. A 391 (1997) 498.
[40] K.-H. Kaiser et al., Nucl. Instr. Meth. A 593 (2008) 159.
[41] H. Olsen and L. C. Maximon, Physical Review 114 (1959) 887.
[42] J.C. McGeorge et al., Eur. Phys. J. A 37 (2008) 129.
[43] C. Rohlof and H. Dutz, Nucl. Instr. Meth. A 526 (2004) 126.
[44] C. Bradtke et al., Nucl. Instr. Meth. A 436 (1999) 430.
[45] O. Rondon, Phys. Rev. C 60 (1999) 35201.
[46] A. Starostin et al., Phys. Rev. C 64 (2001) 55205.
[47] A.R. Gabler et al., Nucl. Instr. Meth. A 346 (1994) 168.
[48] D. Watts, in *Calorimetry in Particle Physics, Proceedings of the 11th Internatinal Conference, Perugia, Italy 2004*, edited by C. Cecchi, P. Cenci, P. Lubrano, and M. Pepe (World Scientific, Singapore, 2005, p. 560).
[49] D. Werthmüller et al., Phys. Rev. C 90 (2014) 015205.
[50] L. Witthauer et al., Eur. Phys. J. A 49 (2013) 154.
[51] S. Agostinelli et al., Nucl. Instr. Meth. A 506 (2003) 250.
[52] M. Lacombe et al., Phys. Lett. B 101 (1981) 139.